Pergamon

Int. J. Heat Mass Transfer. Vol. 40, No. 8, pp. 1853–1861, 1997

0017-9310/97 $17.00+0.00

PII: S0017-9310(96)00247-5

Momentum and heat transfer on a continuous moving surface in a power law fluid

T. G. HOWELL

Department of Chemical Engineering, College of Engineering, The University of Toledo, Toledo, OH 43606, U.S.A.

D. R. JENG†

Department of Mechanical Engineering, College of Engineering, The University of Toledo, Toledo, OH 43606, U.S.A.

and

K. J. DE WITT

Department of Chemical Engineering, College of Engineering, The University of Toledo, Toledo, OH 43606, U.S.A.

(*Received* 12 *December* 1995 *and in final form* 25 *June* 1996)

Abstract—This analysis examines the momentum and heat transfer occurring in the laminar boundary layer on a continuously moving and stretching two-dimensional surface in a non-Newtonian power law fluid. The Merk–Chao series expansion is used to generate ordinary differential equations from the partial differential momentum equation in order to obtain universal velocity functions. For the problem of combined momentum and heat transfer in the boundary layer of the moving sheet, a general power series is used to describe the fluid's velocity and temperature. Examples for a non-linear surface velocity and a linearly stretching surface velocity are provided.

1. INTRODUCTION

In 1961 Sakiadis' developed a new class of boundary layer problems in a series of pioneering papers. Sakiadis [1, 2] analyzed the momentum transfer occurring when a flat surface continuously moves through a quiescent fluid at a constant surface velocity. Both exact and approximate solutions were presented for the laminar flow case with the latter being obtained by the integral method. For turbulent flow, the one-seventh power velocity profile was utilized. In 1967 Sakiadis' work was expanded and experimentally confirmed by Tsou *et al.* [3] who investigated the heat transfer effects of a moving sheet with constant surface velocity and temperature.

In 1966 Erickson *et al.* [4] investigated heat and mass transfer in the laminar boundary layer of a moving flat surface with constant surface velocity and temperature but allowed for suction or injection at the surface. Griffin and Throne [5] confirmed Erickson's theoretical heat transfer coefficients by experimentally observing the thermal boundary layer using the Schmidt shadowgraph method. In 1976 Chida and Katto [6] analyzed conjugate heat transfer in a moving flat plate of constant surface velocity where the flat plate had a finite thickness; consequently, two temperature profiles, one in the solid and one in the fluid, were obtained. Chen and Strobel [7] examined the effect of a buoyancy-induced pressure gradient on the laminar boundary layer of a moving flat plate of constant surface velocity and temperature, and the results compared well to that of Tsou *et al.* [3]. In 1982 Moutsoglou and Bhattacharya [8] extended Sakiadis' turbulent boundary layer work to include non-isothermal flat surfaces using the Van Driest mixing length model to approximate eddy diffusivity.

Abdelhafez [9] numerically investigated skin friction and heat transfer on a flat plate moving with constant velocity through a fluid flowing parallel to the surface using a finite difference method to solve the corresponding Navier–Stokes equations. In 1988 Karwe and Juluria [10] extended Abdelhafez's work to include a flat plate with a finite thickness and mixed convection transport. Chappidi and Gunnerson [11] approached Abdelhafez's problem from an analytical viewpoint and presented closed form expressions that were solved by a Runge–Kutta integral technique and a perturbation procedure. In 1993 Lin *et al.* [12] solved Abdelhafez's problem using the Keller Box method and allowed the fluid to flow in the opposite direction of the moving flat plate.

This class of boundary layer problems was again expanded by Vleggaar [13] who allowed the surface velocity to be a function of distance along the trav-

† Author to whom correspondence should be addressed.

NOMENCLATURE

$a(\xi)$	universal wall velocity gradient, $f_1''(\xi, 0)$
$b(\xi)$	defined in equation (33)
erfc(x)	complimentary error function
k	thermal conductivity
K	consistency index for non-Newtonian viscosity
L	reference length
n	power law exponent
Nu_x	local Nusselt number
Pr	generalized Prandtl number defined in equation (27)
q_s	surface heat flux defined in equation (44)
Re	generalized Reynolds number defined in equation (27)
T	temperature
u	velocity component in the x-direction
U_s	surface velocity
v	velocity component in the y-direction
x	streamwise coordinate measured along surface from slot
x_0	location where surface temperature step-change occurs
y	coordinate normal to surface.

Greek symbols

α	thermal diffusivity
δ_1	displacement thickness defined in equation (40)
δ_2	momentum thickness defined in equation (40)
ζ	transformed dimensionless variable defined in equation (24)
η	dimensionless variable defined in equation (9b)
θ	dimensionless temperature defined in equation (22)
Λ	wedge parameter defined in equation (13)
ξ	dimensionless variable defined in equation (9a)
ρ	fluid density
τ_{yx}	shear stress defined in equation (4).

Subscripts

s	surface conditions
∞	condition of quiescent fluid.

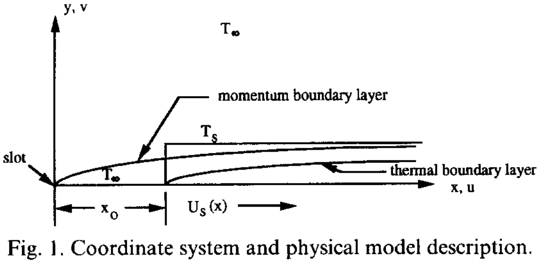

Fig. 1. Coordinate system and physical model description.

ersing coordinate. Vleggaar held the temperature constant, but chose to define the surface velocity as $U = cx$ to compare with his experimental data that showed a non-constant velocity as a polymer monofilament was pulled from a die. In 1986 Jeng *et al.* [14] investigated the momentum and heat transfer for a two-dimensional sheet of arbitrary surface velocity incurring a step change in surface temperature in a quiescent Newtonian fluid. The present work extends the analysis of Jeng *et al.* [14] to a non-Newtonian power law fluid.

2. PROBLEM FORMULATION AND SOLUTION METHOD

The physical problem being examined is shown in Fig. 1. A thin solid surface is extruded from a die slot at $x = y = 0$ on a fixed coordinate system and moves in the x direction with an arbitrary surface velocity, $U_s(x)$. For an incompressible, power law fluid with constant properties moving steadily at a large Reynolds number, the governing boundary layer equations are:

$$\text{continuity} \quad \frac{\partial u}{\partial x} + \frac{\partial v}{\partial y} = 0 \tag{1}$$

$$\text{momentum} \quad u\frac{\partial u}{\partial x} + v\frac{\partial u}{\partial y} = -\frac{1}{\rho}\frac{\partial}{\partial y}(\tau_{yx}) \tag{2}$$

with the boundary conditions

$$u = U_s(x), \quad v = 0 \quad @ \quad y = 0$$
$$u = 0 \quad @ \quad y \to \infty \tag{3}$$

where $U_s(x)$ is the surface velocity. For power law fluids, the shear stress can be defined as

$$\tau_{yx} = -K\left|\frac{\partial u}{\partial y}\right|^{n-1}\frac{\partial u}{\partial y}. \tag{4}$$

For the heat transfer analysis, the surface temperature incurs a step change, i.e. a section of the surface from the slot origin to an arbitrary distance x_0 is isothermal at the fluid temperature T_∞, and for $x > x_0$ the surface temperature is T_s. For a constant property fluid and neglecting viscous dissipation, the governing boundary layer energy equation is:

$$\text{energy} \quad u\frac{\partial T}{\partial x} + v\frac{\partial T}{\partial y} = \alpha\frac{\partial^2 T}{\partial y^2} \tag{5}$$

with

$$T(x,y) = T_\infty + (T_s - T_\infty)H(x-x_0) \quad @ \quad y=0$$

$$T(x,y) = T_\infty \quad @ \quad x = x_0, \quad y>0$$

$$T(x,y) = T_\infty \quad @ \quad y \to \infty \tag{6}$$

where $H(x-x_0)$ is the heavy side unit operator with the values

$$(x-x_0)<0 \quad H(x-x_0)=0$$

$$(x-x_0)>0 \quad H(x-x_0)=1. \tag{7}$$

When $x_0 = 0$, these boundary conditions collapse to that for an isothermal surface at T_s.

The momentum equation and the energy equation are decoupled since the fluid is incompressible, there is no viscous dissipation, and properties are constant. The solution to the momentum equation will be discussed first.

A stream function, $\Psi(x,y)$, defined by

$$u = \frac{\partial \Psi}{\partial y} \quad v = -\frac{\partial \Psi}{\partial x} \tag{8}$$

is introduced to satisfy the continuity equation. Transformations of the original x, y coordinates are achieved by

$$x \to \xi = n\int_0^x U_s^{2n-1}(x)\,\mathrm{d}x \tag{9a}$$

$$y \to \eta = \left[\frac{K}{\rho}(n+1)\xi\right]^{-1/n+1} U_s(x)y. \tag{9b}$$

A dimensionless stream function, $f(\xi,\eta)$, is introduced by

$$\Psi(x,y) = \left[\frac{K}{\rho}(n+1)\xi\right]^{1/n+1} f(\xi,\eta) \tag{10}$$

so that, employing equations (8), (9) and (10), the velocity components become

$$u = U_s(x)f' \tag{11}$$

$$v = -\frac{\left[\frac{K}{\rho}(n+1)\xi\right]^{1/n+1}}{(n+1)\xi} nU_s^{2n-1} \times\left[f + f'\eta(\Lambda-1) + \frac{\partial f}{\partial \xi}(n+1)\xi\right] \tag{12}$$

where Λ is the 'surface velocity parameter' and is defined by

$$\Lambda = \frac{(n+1)\xi}{U_s}\frac{\mathrm{d}U_s}{\mathrm{d}\xi}. \tag{13}$$

Substituting equations (11) and (12) into the momentum equation, the dimensionless stream function, f, satisfies the following transformed momentum equation:

$$f'''|f''|^{n-1} + ff'' - \Lambda(f')^2 = (n+1)\xi\left[f'\frac{\partial^2 f}{\partial\xi\partial\eta} - \frac{\partial f}{\partial \xi}f''\right] \tag{14}$$

with the boundary conditions

$$f=0, \quad \frac{\partial f}{\partial \eta} = 1 \quad @ \quad \eta = 0 \tag{15a}$$

$$\frac{\partial f}{\partial \eta} = 0 \quad @ \quad \eta \to \infty. \tag{15b}$$

Generally, the boundary condition listed in equation (15a) should be $f + (n+1)\xi(\partial f/\partial\xi) = 0$. However, for a non-penetrable surface, the boundary condition $f = 0 \quad @ \quad \eta = 0$ is set and $\partial f/\partial \xi$ vanishes at the surface.

Using the Merk–Chao series expansion, which recognizes the one-to-one relationship between ξ and Λ since both are functions of x only, $f(\xi,\eta,n)$ can be represented in the following form:

$$f(\xi,\eta,\mathrm{n}) = f_0(\Lambda,\eta,n) + (n+1)\xi\frac{\mathrm{d}\Lambda}{\mathrm{d}\xi}f_1(\Lambda,\eta,n) + [(n+1)\xi]^2\frac{\mathrm{d}^2\Lambda}{\mathrm{d}\xi^2}f_2(\Lambda,\eta,n) + \left[(n+1)\xi\frac{\mathrm{d}\Lambda}{\mathrm{d}\xi}\right]^2 f_3(\Lambda,\eta,n)\ldots \tag{16}$$

where the f_is signify universal functions to be solved for specific values of Λ and n, regardless of ξ. Since the first term usually dominates the series expansion, the approximation $|f''|^{n-1} \approx |f_0''|^{n-1}$ is made as done by Chang [15]. This approximation can be proved valid by inspection of results.

Inserting equation (16) into equation (14) and collecting terms free of $\mathrm{d}\Lambda/\mathrm{d}\xi$ and then terms containing

$$(n+1)\xi\frac{\mathrm{d}\Lambda}{\mathrm{d}\xi}, \quad [(n+1)\xi]^2\frac{\mathrm{d}^2\Lambda}{\mathrm{d}\xi^2}, \quad \left[(n+1)\xi\frac{\mathrm{d}\Lambda}{\mathrm{d}\xi}\right]^2, \ldots,$$

a series of ordinary differential equations is obtained. The first equation of the series is

$$f_0'''|f_0''|^{n-1} + f_0f_0'' - \Lambda(f_0')^2 = 0 \tag{17a}$$

with

$$f_0(\Lambda,\eta,n) = 0, \quad f_0'(\Lambda,\eta,n) = 1 \quad @ \quad \eta = 0 \tag{17b}$$

$$f_0'(\Lambda,\eta,n) = 0 \quad @ \quad \eta \to \infty. \tag{17c}$$

The second, third, and fourth equations in the series are

$$f_1'''|f_0''|^{n-1} + f_0f_1'' + (n+2)f_0''f_1 - 2\left(\Lambda + \frac{n+1}{2}\right)f_0'f_1' = \frac{\partial f_0'}{\partial \Lambda}f_0' - \frac{\partial f_0}{\partial \Lambda}f_0'' \tag{18}$$

$$f_2'''|f_0''|^{n-1}+f_0f_2''+(2n+3)f_0''f_2-2(\Lambda+n+1)f_0'f_2' = f_1'f_0'-f_1f_0'' \quad (19)$$

$$f_3'''|f_0''|^{n-1}+f_0f_3''+(2n+3)f_0''f_3+(n+2)f_1''f_1 -(\Lambda+n+1)(2f_0'f_3'+(f_1')^2) = \left(\frac{\partial f_1'}{\partial\Lambda}f_0'-\frac{\partial f_0}{\partial\Lambda}f_1''\right)+\left(\frac{\partial f_0'}{\partial\Lambda}f_1'-\frac{\partial f_1}{\partial\Lambda}f_0''\right) \quad (20)$$

with

$$f_i(\Lambda,\eta,n)=f_i'(\Lambda,\eta,n)=0 \quad @ \quad \eta=0 \quad (21a)$$

$$f_i'(\Lambda,\eta,n)=0 \quad @ \quad \eta\to\infty \quad (21b)$$

where $i = 1, 2$ and 3.

It should be noted that the above coupled ordinary differential equations reduce to the corresponding equations of Jeng *et al.* [14] when $n = 1.0$. It should also be noted that the f_is ($i = 0, 1, 2$ and 3) represent universal functions that can be tabulated once and for all for any specific Λ and n.

In order to solve the energy equation for a step change in surface temperature, further transformations are needed:

$$\theta=\frac{T-T_\infty}{T_s-T_\infty} \quad (22)$$

$$\xi\to\chi=\left[1-\left(\frac{\xi_0}{\xi}\right)^c\right]^{1/2} \quad (23)$$

$$\eta\to\zeta=b(\xi)\frac{\eta}{\chi} \quad (24)$$

where

$$\xi_0=n\int_0^{x_0}U_s^{2n-1}(x)\,\mathrm{d}x \quad (25)$$

as was done by Jeng *et al.* [14].

The actual expressions for c and $b(\xi)$ are deferred until a set of ordinary differential equations is obtained; however, c must be a constant and $b(\xi)$ has to be defined such that the solution of the set of equations can be expressed as universal functions, independent of the problem's geometry.

Upon substituting equations (22), (23), and (24) into equation (5), the thermal energy equation becomes

$$\frac{\partial^2\theta}{\partial\zeta^2}+\frac{\partial\theta}{\partial\zeta}\frac{A}{b}\left\{\chi\left(f+((n+1)\xi\frac{\partial f}{\partial\xi}\right)+\left[\frac{c}{2b}(1-\chi^2)-\frac{\xi\chi^2}{b^2}\frac{\mathrm{d}b}{\mathrm{d}\xi}\right](n+1)\zeta\frac{\partial f}{\partial\eta}\right\}+\frac{A(n+1)c}{2b^2}(\chi^3-\chi)\frac{\partial f}{\partial\eta}\frac{\partial\theta}{\partial\chi}=0 \quad (26)$$

where

$$A=nPr\left[\frac{(n+1)\xi}{U_s^{2n-1}L}\right]^{1-n/n+1}.$$

The generalized Pr and Re numbers are defined by the following relations:

$$Pr=\frac{\rho c_p U_s L}{k(Re)^{2/n+1}} \quad Re=\frac{\rho U_s^{2-n}L^n}{K} \quad (27)$$

with

$$\theta(\chi,\zeta)=1 \quad @ \quad \zeta=0 \quad (28a)$$

$$\theta(\chi,\zeta)=0 \quad @ \quad \zeta\to\infty. \quad (28b)$$

In order to obtain a solution to equation (26), the velocity functions, namely f, $\partial f/\partial\xi$ and $\partial f/\partial\eta$ must be represented in a series. Consequently, the dimensionless stream function is defined by

$$f(\xi,\eta)=\sum_{j=1}^{\infty}a_j\frac{\eta^j}{j!}=\frac{\zeta}{b}\chi+\frac{a_2\zeta^2}{2!b^2}\chi^2+\frac{a_3\zeta^3}{3!b^3}\chi^3+\frac{a_4\zeta^4}{4!b^4}\chi^4+\cdots \quad (29)$$

with the boundary conditions stated in equation (15). Using equation (29) in equation (14), rearranging, and collecting like powers of η, the first five coefficients of a_j in equation (29) become

$$a_1=1;\quad a_2=f''(\eta=0)=a;$$

$$a_3=\Lambda|a|^{1-n};\quad a_4=|a|^{1-n}[a(2\Lambda-1)+(n+1)\xi a']$$

$$a_5=2\Lambda[|a|^{2-2n}(\Lambda-1)]+|a|^{3-n}(2\Lambda-1)+(n+1)\xi[a'(\Lambda(n-1)|a|^{1-2n}-|a|^{2n})+\Lambda'|a|^{2-2n}]. \quad (30)$$

The series solution to the transformed energy equation was sought in the following series:

$$\theta=\sum_{m=0}^{\infty}\theta_m(\xi,\zeta)\chi^m \quad (31)$$

and

$$\theta_0(\xi,\zeta)=1,\quad \theta_i(\xi,\zeta)=0 \quad @ \quad \zeta=0 \quad (32a)$$

$$\theta_0(\xi,\zeta)=0,\quad \theta_i(\xi,\zeta)=0 \quad @ \quad \zeta\to\infty \quad (32b)$$

where $i = 1, 2$, and 3.

Inserting equations (29) and (31) into equation (26) and collecting like powers of χ, a set of linear partial differential equations are obtained. In order to simplify this set of equations, it is necessary to define

$$c=\frac{2}{n+1},\quad b(\xi)=\sqrt{A},\quad \theta_1=\frac{a}{b}\bar\theta_1$$

$$\theta_2=\frac{a^2}{b^2}\bar\theta_{2,1}+\frac{a_3}{2b^2}\bar\theta_{2,2}+\left[\frac{A\xi}{b^3}(n+1)\frac{\mathrm{d}b}{\mathrm{d}\xi}\right]\bar\theta_{2,3}$$

$$\theta_3=\frac{a^3}{b^3}\bar\theta_{3,1}+\frac{aa_3}{2b^3}\bar\theta_{3,2}+\frac{a}{b}\bar\theta_{3,3}+\left[\frac{A}{2b^3}\times(a+(n+1)\xi a')-\frac{A\xi a}{b^4}(n+1)\frac{\mathrm{d}b}{\mathrm{d}\xi}\right]\bar\theta_{3,4}+\frac{a_4}{6b^3}\bar\theta_{3,5}+\left[\frac{A\xi a}{b^4}(n+1)\frac{\mathrm{d}b}{\mathrm{d}\xi}\right]\bar\theta_{3,6}. \quad (33)$$

Employing equation (33), equation (26) reduces to the following equations:

$$\theta_0''+\zeta\theta_0' = 0 \tag{34}$$

$$\bar{\theta}_1''+\zeta\bar{\theta}_1'-\bar{\theta}_1 = -\zeta^2\theta_0' \tag{35}$$

$$\bar{\theta}_{2,1}''+\zeta\bar{\theta}_{2,1}'-2\bar{\theta}_{2,1} = -\zeta^2\bar{\theta}_1'+\zeta\bar{\theta}_1 \tag{36a}$$

$$\bar{\theta}_{2,2}''+\zeta\bar{\theta}_{2,2}'-2\bar{\theta}_{2,2} = -\zeta^3\theta_0' \tag{36b}$$

$$\bar{\theta}_{2,3}''+\zeta\bar{\theta}_{2,3}'-2\bar{\theta}_{2,3} = \zeta\theta_0' \tag{36c}$$

$$\bar{\theta}_{3,1}''+\zeta\bar{\theta}_{3,1}'-3\bar{\theta}_{3,1} = -\zeta^2\bar{\theta}_{2,1}'+2\zeta\bar{\theta}_{2,1} \tag{37a}$$

$$\bar{\theta}_{3,2}''+\zeta\bar{\theta}_{3,2}'+3\bar{\theta}_{3,2} = -\zeta^3\bar{\theta}_1'-\zeta^2\bar{\theta}_{2,2}'+2\zeta\bar{\theta}_{2,2}+\zeta^2\bar{\theta}_1 \tag{37b}$$

$$\bar{\theta}_{3,3}''+\zeta\bar{\theta}_{3,3}'-3\bar{\theta}_{3,3} = -\bar{\theta}_1+\zeta^2\theta_0' \tag{37c}$$

$$\bar{\theta}_{3,4}''+\zeta\bar{\theta}_{3,4}'-3\bar{\theta}_{3,4} = -\zeta^2\theta_0' \tag{37d}$$

$$\bar{\theta}_{3,5}''+\zeta\bar{\theta}_{3,5}'-3\bar{\theta}_{3,5} = -\zeta^4\theta_0' \tag{37e}$$

$$\bar{\theta}_{3,6}''+\zeta\bar{\theta}_{3,6}'-3\bar{\theta}_{3,6} = -\zeta^2\bar{\theta}_{2,3}'+2\zeta\bar{\theta}_{2,3}+\zeta\bar{\theta}_1' \tag{37f}$$

with the corresponding boundary conditions:

$$\theta_0(\xi,\zeta) = 1,\quad \bar{\theta}_1(\xi,\zeta) = \bar{\theta}_{m,n}(\xi,\zeta) = 0 \quad @ \quad \zeta = 0$$
$$\theta_0(\xi,\zeta) = 0,\quad \bar{\theta}_1(\xi,\zeta) = \bar{\theta}_{m,n}(\xi,\zeta) = 0 \quad @ \quad \zeta \to \infty \tag{38}$$

where the primes denote partial differentiation with respect to ζ. It is worth noting that Jeng *et al.* [14] incorrectly defined equation (37c) by using $\cdots+\zeta\theta_0'$ on the right hand side instead of $\cdots+\zeta^2\theta_0'$ as in the present case. This difference can be quantified through direct comparison later.

3. FORMULA RELATING TO MOMENTUM AND HEAT TRANSFER

The calculation of the local friction coefficient and Nusselt number and the development of the displacement and momentum thickness, becomes a simple matter when using the solutions for f_i and θ_i. The only required value is the surface velocity $U_s(x)$, which may be obtained from experimentation.

Using universal functions, the local friction coefficient can be expressed as

$$c_f = \frac{\tau_{yx}|_{y=0}}{\frac{1}{2}\rho U_s^2} = -\frac{2}{Re^{1/n+1}}\left[\frac{U_s^{2n-1}L}{(n+1)\xi}\right]^{n/n+1}|f_0''|^{n-1}(\Lambda,0)$$
$$\times\left\{f_0''(\Lambda,0)+(n+1)\xi\frac{d\Lambda}{d\xi}f_1''(\Lambda,0)+[(n+1)\xi]^2\right.$$
$$\left.\times\frac{d^2\Lambda}{d\xi^2}f_2''(\Lambda,0)+\cdots\right\}. \tag{39}$$

The displacement and momentum thicknesses for a continuous, two-dimensional moving sheet are given by

$$\delta_1 = \frac{1}{U_s}\int_0^{\eta_\infty} u\,dy \quad \delta_2 = \frac{1}{U_s^2}\int_0^{\eta_\infty} u^2\,dy \tag{40}$$

and

$$\delta_1 = \frac{\left[\frac{K}{\rho}(n+1)\xi\right]^{1/n+1}}{U_s}\left\{f_0(\Lambda,\eta_\infty)\right.$$
$$+(n+1)\xi\frac{d\Lambda}{d\xi}f_1(\Lambda,\eta_\infty)$$
$$\left.+[(n+1)\xi]^2\frac{d^2\Lambda}{d\xi^2}f_2(\Lambda,\eta_\infty)+\cdots\right\} \tag{41}$$

$$\delta_2 = \frac{\left[\frac{K}{\rho}(n+1)\xi\right]^{1/n+1}}{U_s}\left\{I_1(\Lambda)+(n+1)\xi\frac{d\Lambda}{d\xi}I_2(\Lambda)\right.$$
$$\left.+[(n+1)\xi]^2\frac{d^2\Lambda}{d\xi^2}I_3(\Lambda)+\cdots\right\} \tag{42}$$

where

$$I_1 = \int_0^{\eta_\infty}(f_0')^2\,d\eta \quad I_2 = 2\int_0^{\eta_\infty}f_0'f_1'\,d\eta$$
$$I_3 = 2\int_0^{\eta_\infty}f_0'f_2'\,d\eta. \tag{43}$$

Evaluating the integrals in equation (43) and inserting the values into the momentum thickness equation becomes a relatively easy procedure. Values needed to calculate the displacement thickness are given in ref. [16].

The expression for the local surface heat flux for a step change in temperature is given by

$$q_s = -k\frac{\partial T}{\partial y}\bigg|_{y=0}$$
$$= \frac{k(T_s-T_\infty)}{\chi}\left[\frac{nPrRe^{2/n+1}U_s^{2n-1}}{(n+1)\xi L}\right]^{1/2}\left(-\frac{\partial\theta}{\partial\zeta}\right)\bigg|_{\zeta=0} \tag{44}$$

and the Nusselt number is defined by

$$Nu = \frac{q_sL}{k(T_s-T_\infty)}$$
$$= \frac{1}{\chi}\left[\frac{nPrRe^{2/n+1}U_s^{2n-1}L}{(n+1)\xi}\right]^{1/2}\left(-\frac{\partial\theta}{\partial\zeta}\right)\bigg|_{\zeta=0} \tag{45}$$

where

$$\left(-\frac{\partial\theta}{\partial\zeta}\right)\Bigg|_{\zeta=0} = 0.79788+\frac{0.25a}{b}\chi$$
$$+\left[\frac{0.09974a_3-0.12467a^2}{b^2}\right.$$
$$\left.-0.19947\left[\frac{\xi}{b}(n+1)\frac{\mathrm{d}b}{\mathrm{d}\xi}\right]\right]\chi^2$$
$$+\left[\frac{0.11719a^3+0.03125a_4-0.14063aa_3}{b^3}\right.$$
$$\left.+0.0625\left[\frac{(n+1)\xi a'}{b}-\frac{\xi a}{b^2}(n+1)\frac{\mathrm{d}b}{\mathrm{d}\xi}\right]\right]\chi^3+\cdots. \quad (46)$$

The dimensionless temperature profile can now be written more precisely as

$$\theta(\Lambda,\zeta,\chi) = \theta_0(\zeta)+\frac{a}{b}\bar{\theta}_1(\zeta)\chi+\left[\frac{a^2}{b^2}\bar{\theta}_{2,1}(\zeta)\right.$$
$$\left.+\frac{a_3}{2b^2}\bar{\theta}_{2,2}(\zeta)+\left[\frac{\xi}{b}(n+1)\frac{\mathrm{d}b}{\mathrm{d}\xi}\right]\bar{\theta}_{2,3}(\zeta)\right]\chi^2$$
$$+\left[\frac{a^3}{b^3}\bar{\theta}_{3,1}(\zeta)+\frac{aa_3}{2b^3}\bar{\theta}_{3,2}(\zeta)+\frac{a}{b}\bar{\theta}_{3,3}(\zeta)\right.$$
$$+\left[\frac{1}{2b}(a+(n+1)\xi a')-\frac{\xi a}{b^2}(n+1)\frac{\mathrm{d}b}{\mathrm{d}\xi}\right]$$
$$\times\bar{\theta}_{3,4}(\zeta)+\frac{a_4}{6b^3}\bar{\theta}_{3,5}(\zeta)+\left[\frac{\xi a}{b^2}(n+1)\frac{\mathrm{d}b}{\mathrm{d}\xi}\right]$$
$$\left.\times\bar{\theta}_{3,6}(\zeta)\right]\chi^3+\cdots. \quad (47)$$

The above analysis uses the first four terms, but terms of higher order may be obtained by a simple calculation. The accuracy of using a finite number of terms in the series depends on the convergency of the series. However, convergence was excellent in the above analysis.

4. NUMERICAL SOLUTIONS AND ACCURACY ESTIMATION

The differential equations obtained for f_i ($i = 0, 1, 2$ and 3) were numerically integrated by a fourth order Runge–Kutta integration technique using double precision. Data for nine values of n ranging from 0.3 to 1.9 and for six values of Λ ranging from -0.10 to 1.0 have been computed and recorded.

High accuracy for the f_0 solutions is necessary since f_1 and f_2 are dependent on the f_0 results. The integration step size, $\Delta\eta$, represents a compromise between truncation error and computation time. This step size, along with the convergence criteria, had to be varied with n to control computation time. The iterations were continued until the conditions listed in Table 1 were met. For example, when $n = 1.3$, convergence was considered reached when $|f'_0(\eta_\infty)| < 1.0\times10^{-8}$ where η_∞ denotes some large value of η. Trends in boundary layer thickness are also shown in Table 1. As n increases, the η_∞ required to reach quiescent fluid decreases, indicating the momentum boundary layer thickness decreases with increasing power law exponent. The results obtained in this manner compare well with those published by Jeng *et al.* [14]. A complete listing of all surface derivatives may be found in Table 2.

Table 1. Convergence criteria for numerical integration technique

n	$\lvert f'_0(\eta_\infty)\rvert$	$\lvert f'_1(\eta_\infty)\rvert$	$\lvert f'_2(\eta_\infty)\rvert$	η_∞	Step size
0.3	1.0×10^{-5}	1.0×10^{-5}	1.0×10^{-4}	550	0.02
0.5	1.0×10^{-6}	1.0×10^{-6}	1.0×10^{-6}	550	0.02
0.7	1.0×10^{-8}	1.0×10^{-8}	1.0×10^{-8}	470	0.02
0.9	1.0×10^{-10}	1.0×10^{-8}	1.0×10^{-8}	70	0.01
1.0	1.0×10^{-10}	1.0×10^{-8}	1.0×10^{-8}	21	0.01
1.1	1.0×10^{-10}	1.0×10^{-8}	1.0×10^{-8}	9.5	0.01
1.3	1.0×10^{-8}	1.0×10^{-8}	1.0×10^{-8}	4.2	0.01
1.5	1.0×10^{-6}	1.0×10^{-6}	1.0×10^{-6}	2.85	0.01
1.7	1.0×10^{-6}	1.0×10^{-6}	1.0×10^{-6}	2.27	0.01
1.9	1.0×10^{-6}	1.0×10^{-3}	1.0×10^{-3}	1.95	0.01

High accuracy is also required for the temperature function θ_0 for the same reason as that given for f_0. However, the θ_0 equation has a closed form solution given by

$$\theta_0(\xi,\zeta) = \operatorname{erfc}\left(\frac{\zeta}{\sqrt{2}}\right) \quad (48)$$

with the surface derivative

$$\theta'_0(\xi,\zeta=0) = -\sqrt{\frac{2}{\pi}} = -0.797885 \quad (49)$$

An Adams–Moulten predictor–corrector technique was used for the integration of the $\bar{\theta}_1$ and $\bar{\theta}_{m,n}$ equations with a fourth order Runge–Kutta technique serving as a start-up method. The iterations would continue until the following condition was met:

$$|\bar{\theta}_{m,n}(\zeta\to\infty)| < 10^{-5} \quad (50)$$

The numerical solutions to equations (35)–(37) are available in ref. [16]. The surface derivatives of these functions are required in order to evaluate the surface heat flux and are

$$\bar{\theta}'_1(\zeta=0) = -0.250000 \quad \bar{\theta}'_{3,2}(\zeta=0) = 0.281250$$
$$\bar{\theta}'_{2,1}(\zeta=0) = 0.124669 \quad \bar{\theta}'_{3,3}(\zeta=0) = 0.062500$$
$$\bar{\theta}'_{2,2}(\zeta=0) = -0.199471 \quad \bar{\theta}'_{3,4}(\zeta=0) = -0.125000$$
$$\bar{\theta}'_{2,3}(\zeta=0) = 0.199471 \quad \bar{\theta}'_{3,5}(\zeta=0) = -0.187500$$
$$\bar{\theta}'_{3,1}(\zeta=0) = -0.117187 \quad \bar{\theta}'_{3,5}(\zeta=0) = -0.062500. \quad (51)$$

Table 2. Surface derivative comparison with ref. [14]

Λ	$f_0''(0)$		$f_1''(0)\times 10$		$f_2''(0)\times 100$	
	Present	Ref. [14]	Present	Ref. [14]	Present	Ref. [14]
−0.10	−0.5815786	−0.5815786	0.6086720	0.6086720	−0.8706994	−0.8706994
0.00	−0.6275549	−0.6275549	0.5519511	0.5519510	−0.7698453	−0.7698450
0.25	−0.7337875	−0.7337875	0.4412525	0.4412525	−0.5787687	−0.5787689
0.50	−0.8299459	−0.8299459	0.3615800	0.3615800	−0.4470959	−0.4470959
0.75	−0.9181773	−0.9181774	0.3022943	0.3022944	−0.3531981	−0.3531983
1.00	−1.0000000	−1.0000000	0.2569553	0.2569556	−0.2483160	−0.2843165

5. APPLICATIONS

In this section, two examples using different surface velocity distributions will be given in order to demonstrate the usefulness and the accuracy of the series solution presented in this paper. They include the power law surface velocity and the linearly stretching surface velocity with a non-zero slot velocity.

5.1. *Surface velocity proportional to a power of distance measured from the slot*

Consider the following surface velocity:

$$U_s(x) = cx^m \tag{52}$$

where c and m are constants. Substituting this surface velocity into equations (9a) and (13), ξ and Λ become

$$\xi = \frac{nc^{2n-1}x^{m(2n-1)+1}}{m(2n-1)+1} \quad \Lambda = \frac{m(n+1)}{m(2n-1)+1}. \tag{53}$$

For a given n, Λ is a constant; therefore,

$$\frac{d\Lambda}{d\xi} = \frac{d^2\Lambda}{d\xi^2} = \cdots = 0.$$

With the Λ derivatives equal to zero, the local friction coefficient for this flow becomes

$$\frac{1}{2}c_f Re_x^{1/n+1} = \left[\frac{m(2n-1)+1}{n(n+1)}\right]^{n/n+1}\{|f_0''(\Lambda,0)|^n\} \tag{54}$$

where

$$Re_x = \frac{\rho c^{2-n}x^{m(2-n)+n}}{K}.$$

If the flow incurs a step-change in temperature at x_0, the local Nusselt number can be calculated with the following equation:

$$Nu_x Re_x^{-1/2} = \left[\frac{Pr(m(2n-1)+1)}{(n+1)}\right]^{1/2}\frac{\left(-\dfrac{\partial\theta}{\partial\zeta}\right)\Big|_{\zeta=0}}{\chi}. \tag{55}$$

5.2. *Linearly stretched surface with non-zero slot velocity*

As previously mentioned, the disadvantage of the non-linear surface velocity is the zero velocity at the origin; however, if the surface velocity is taken to be

$$U_s(x) = U_0\left(1+\frac{x}{L}\right) \tag{56}$$

where L is the inverse of the absolute magnitude to the velocity gradient, one can see the more realistic non-zero velocity at the slot. Using this surface velocity, ξ, Λ and Λs derivatives become

$$\begin{aligned}
\xi &= \frac{1}{2}U_0^{2n-1}L\left[\left(1+\frac{x}{L}\right)^{2n}-1\right] \\
\Lambda &= \frac{(n+1)}{2n}\left[1-\left(1+\frac{x}{L}\right)^{-2n}\right] \\
(n+1)\xi\frac{\partial\Lambda}{\partial\xi} &= \frac{(n+1)^2}{2n}\frac{\left[\left(1+\frac{x}{L}\right)^{2n}-1\right]}{\left(1+\frac{x}{L}\right)^{4n}} \\
(n+1)^2\xi^2\frac{\partial^2\Lambda}{\partial\xi^2} &= -\frac{(n+1)^3}{n}\frac{\left[\left(1+\frac{x}{L}\right)^{2n}-1\right]^2}{\left(1+\frac{x}{L}\right)^{6n}}.
\end{aligned} \tag{57}$$

The variation of dimensionless velocity profiles with n for a linearly stretched surface at $x/L = 0.5$ can be seen in Fig. 2. This figure also illustrates the relative boundary layer thicknesses for non-Newtonian fluids of different power law exponents. For a non-Newtonian fluid with a power law exponent of 1.5, the boundary layer is relatively thin (f' approaches zero quickly). However, if $n = 0.5$, the boundary layer is relatively thick by comparison.

The local friction coefficient for a linearly stretched surface becomes

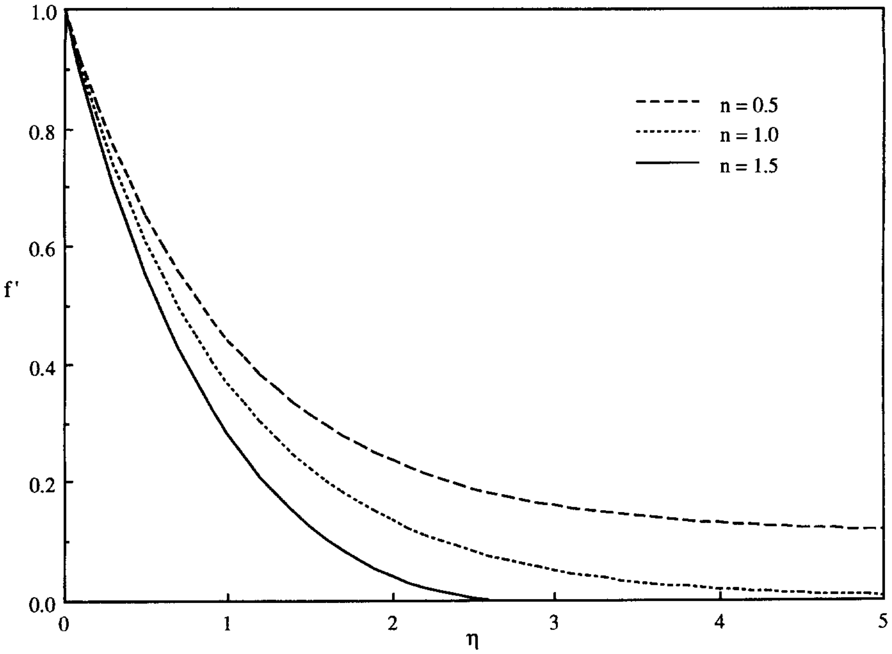

Fig. 2. Variation of dimensionless velocity profiles with n for linearly stretched surface velocity at $x/L = 0.5$.

$$\frac{1}{2}c_f Re_x^{1/n+1} = -\left[\frac{\frac{2x}{L}\left(1+\frac{x}{L}\right)^{2n-1}}{(n+1)\left[\left(1+\frac{x}{L}\right)^{2n}-1\right]}\right]^{n/n+1}$$

$$|f_0''(\Lambda,0)|^{n-1}\left\{f_0''(\Lambda,0)+(n+1)\xi\frac{d\Lambda}{d\xi}f_1''(\Lambda,0)+\cdots\right\} \quad (58a)$$

where

$$Re_x = \frac{\rho U_0^{2-n}\left(1+\frac{x}{L}\right)^{2-n}x^n}{K}. \quad (58b)$$

If the flow incurs a step-change in temperature at x_0, the local Nusselt number can be calculated with the following equation:

$$Nu_x Re_x^{-1/n+1} = \left[\frac{2nPr_x\left(1+\frac{x}{L}\right)^{2n-1}\frac{x}{L}}{(n+1)\left[\left(1+\frac{x}{L}\right)^{2n}-1\right]}\right]^{1/2}\frac{\left(-\left.\frac{\partial\theta}{\partial\zeta}\right)\right|_{\zeta=0}}{\chi} \quad (59a)$$

where

$$Re_x = \frac{\rho U_s^{2-n}x^n}{K} \quad \text{and} \quad Pr_x = \frac{\rho c_p U_s x}{k(Re_x)^{2/n+1}}. \quad (59b)$$

For tabulation, equation (59a) can be rewritten as

$$Nu_x Re_x^{-1/2} = \left[\frac{2nPr\left(1+\frac{x}{L}\right)^{2n}\frac{x}{L}}{(n+1)\left[\left(1+\frac{x}{L}\right)^{2n}-1\right]}\right]^{1/2}\frac{\left(-\left.\frac{\partial\theta}{\partial\zeta}\right)\right|_{\zeta=0}}{\chi} \quad (60a)$$

where

$$Re_x = \frac{\rho U_0 x}{K} \quad \text{and} \quad Pr = \frac{K}{\rho\alpha}. \quad (60b)$$

Table 3 was generated using equation (60a). A comparison of $Nu_x Re_x^{-1/2}$ between ref. [14] and the present study for the Newtonian case finds a difference of approximately 6%. This difference can be attributed to the error found in equation (37c). It is worth noting that Kim and Jeng [17] have already presented results for $Nu_x Re_x^{-1/2}$ for non-Newtonian power law fluids. In that analysis, only f_0'' was used for the velocity gradient at the surface, whereas the present study used the first three terms. Also, the equation used by Kim and Jeng [17] to generate a table similar to Table 3 had the same error that appeared in Jeng et al. [14]. Consequently, an in-depth comparison of Kim and Jeng [17] and the present study is not presented here.

6. CONCLUSIONS

The problem of analyzing the momentum and heat transfer in the laminar boundary layer of a continuous two-dimensional sheet moving through a quiescent power law fluid was solved by the application of the

Table 3. $Nu_x Re_x^{-1/2}$ comparison for linearly stretched isothermal surface ($\chi = 1$) with ref. [14]

	$Pr = 0.7$						
	$n = 1.0$			$n = 0.5$		$n = 1.5$	
Λ	x/L	Present	Ref. [14]	x/L	Present	x/L	Present
0.1	0.0541	0.32150	0.34336	0.0714	0.46321	0.04354	0.21677
0.3	0.1952	0.34963	0.36684	0.2500	0.49665	0.1604	0.23642
0.5	0.4142	0.38334	0.40373	0.5000	0.53516	0.3572	0.25955
0.7	0.8257	0.44378	0.47048	0.8750	0.59425	0.8420	0.30872

Merk–Chao series expansion method. Sakiadis' moving surface problem had been studied by many investigators; however, this marks the first time that the problem has been solved for a non-Newtonian power law fluid with more than a one term Merk–Chao series analysis.

Appropriate coordinate transformations and series expansions of the velocity function, f, and temperature, θ, were presented. The set of ordinary differential equations arising from the Merk–Chao series were derived and solved using numerical techniques, which are detailed in the text. The singularity problems that arise were avoided using l'Hopital's rule and limiting the investigation to non-Newtonian fluids whose power law index were less than two.

Comparisons made with Jeng *et al.* [14] for a Newtonian fluid illustrated an error located in the analysis of Jeng *et al.* [14]. Comparisons made with Kim and Jeng [17] for non-Newtonian fluids had similar discrepancies. For future work, one could use Duhamel's integral to predict the solid surface temperature profile of the moving surface by using the series expansion of the surface temperature universal functions as the kernel.

The Merk–Chao series expansion is a useful method to solve difficult transport problems in that simple transformations and universal functions are used to solve the fundamental differential equations regardless of geometry.

Acknowledgements—The authors express their thanks to the NASA Lewis Research Center for graduate student support for T. G. Howell under Grant NAG 3-577. Paul F. Penko was the grant monitor.

REFERENCES

1. Sakiadis, B. C., Boundary-layer behavior on continuous solid surfaces: I. Boundary-layer equations for two-dimensional and axisymmetric flow. *A.I.Ch.E. Journal*, 1961, **7,** 26–28.
2. Sakiadis, B. C., Boundary-layer behavior on continuous solid surfaces: II. Boundary-layer on a continuous flat surface. *A.I.Ch.E. Journal*, 1961, **7,** 221–225.
3. Tsou, F. K., Sparrow, E. M. and Goldstein, R. J., Flow and heat transfer in the boundary-layer on a continuous moving surface. *International Journal of Heat and Mass Transfer*, 1967, **10,** 219–235.
4. Erickson, L. E., Fan, L. T. and Fox, V. G., Heat and mass transfer on a moving continuous flat plate with suction or injection. *Industrial Engineering Chemistry Fundamentals*, 1966, **5,** 19–25.
5. Griffin, J. F. and Throne, J. L., On thermal boundary layer growth on continuous moving belts. *A.I.Ch.E. Journal*, 1967, **13,** 1210–1211.
6. Chida, K. and Katto, Y., Conjugate heat transfer of continuously moving surfaces. *International Journal of Heat and Mass Transfer*, 1976, **19,** 461–469.
7. Chen, T. S. and Strobel, F. A., Buoyancy effects in boundary layer adjacent to a continuous, moving horizontal flat plate. *Journal of Heat Transfer*, 1980, **102,** 170–172.
8. Moutsoglou, A. and Bhattacharya, A. K., Laminar and turbulent boundary layers on moving, nonisothermal continuous flat surfaces. *Journal of Heat Transfer*, 1982, **104,** 707–714.
9. Abdelhafez, T. A., Skin friction and heat transfer on a continuous flat surface moving in a parallel free stream. *International Journal of Heat and Mass Transfer*, 1985, **28,** 1234–1237.
10. Karwe, M. V. and Jaluria, Y., Fluid flow and mixed convection transport from a moving plate in rolling and extrusion processes. *Journal of Heat Transfer*, 1988, **110,** 655–661.
11. Chappidi, P. R. and Gunnerson, F. S., Analysis of heat and momentum transfer along a moving surface. *International Journal of Heat and Mass Transfer*, 1989, **32,** 1383–1386.
12. Lin, H. T., Wu, K. Y. and Hoh, H. L., Mixed convection from an isothermal horizontal plate moving in parallel or reversely to a free stream. *International Journal of Heat and Mass Transfer*, 1993, **36,** 3547–3554.
13. Vleggaar, J., Laminar boundary-layer behavior on continuous, accelerating surfaces. *Chemical Engineering Science*, 1977, **32,** 1517–1525.
14. Jeng, D. R., Chang, T. A. and DeWitt, K. J., Momentum and heat transfer on a continuous moving surface. *Journal of Heat Transfer*, 1986, **108,** 532–539.
15. Chang, T. A., Laminar natural convection of non-Newtonian fluids over a two-dimensional or axisymmetric body with uniform surface temperature. Ph.D. thesis, University of Toledo, Toledo, Ohio, 1986.
16. Howell, T. G., Analysis in theoretical and experimental fluid flow. M.Sc. thesis, University of Toledo, Toledo, Ohio, 1996.
17. Kim, H. W. and Jeng, D. R., Convective heat transfer from a continuously moving flat surface to a non-Newtonian fluid. In *Proceedings of the Fifth International Conference of Math and Computer Modeling*, San Francisco, California, 1994.